EUSTATIC CONTROL ON ALLUVIAL SEQUENCE STRATIGRAPHY: A POSSIBLE EXAMPLE FROM THE CRETACEOUS–TERTIARY TRANSITION OF THE TORNILLO BASIN, BIG BEND NATIONAL PARK, WEST TEXAS, U.S.A.

STACY C. ATCHLEY, LEE C. NORDT, AND STEPHEN I. DWORKIN
Baylor University, Department of Geology, P.O. Box 97354, Waco, Texas 76798-7354, U.S.A.
e-mail: stacy_atchley@baylor.edu

ABSTRACT: **Paleosol-bearing alluvial strata of latest Cretaceous and earliest Tertiary age are continuously exposed along Dawson Creek, in Big Bend National Park, west Texas, U.S.A., and exhibit a three-tier hierarchy of depositional cyclicity. Meter-scale, fluvial aggradational cycles (FACs) occur as fining-upward successions that are gradationally overlain by paleosols or are sharply overlain by the coarser-grained base of the succeeding FAC without an intervening paleosol. FACs stack into decameter-scale, fluvial aggradational cycle sets (FAC sets) that also fine upward, and from base to top contain either a gradual upsection increase in soil maturity and soil drainage or a somewhat symmetrical pattern of increasing and decreasing paleosol maturity. Longer-period trends of FAC thickness, lithologic proportions, paleosol maturity, and paleosol drainage indicate that two complete, and two partial, hectometer-scale fluvial sequences occur within the study interval. From base to top, each sequence is characterized by an asymmetric increase and decrease in FAC thickness, a decrease in the proportion of sand-prone fluvial facies, an increase in paleosol maturity, and better paleosol drainage.**

Whereas FACs and FAC sets are interpreted to record cyclic episodes of channel avulsion and stability, and longer-term avulsive channel drift within the alluvial valley, respectively, fluvial sequences may coincide with third-order sea-level changes within the North American Western Interior Seaway. As such, the Cretaceous–Tertiary (K–T) transition within the Tornillo Basin may provide an example of megascale stratigraphic cyclicity that is controlled by eustatic sea level within a fully fluvial succession. Thickening and thinning successions of FACs record a third-order period of accelerating (transgressive-equivalent) and decelerating (highstand-equivalent) base-level rise, and subsequent base-level fall (falling stage- to lowstand-equivalent). Sequence boundaries are placed at the sharp inflection between thinning and thickening FACs. Sand-prone facies and immature, more poorly-drained paleosols are associated with the transgressive-equivalent portion of each sequence, and mudrock-dominated overbank facies and their associated mature, well-drained paleosols are associated with the highstand- and falling stage-equivalent.

INTRODUCTION

Thick, relatively conformable alluvial successions and associated paleosols have been suggested to contain a hierarchical record of cyclic sediment accumulation produced in response to the combined effects of autogenic and allogenic processes (e.g., Beerbower 1964; Bridge and Leeder 1979; Bridge 1984; Kraus 1987, 1999; Kraus and Aslan 1999; Shanley and McCabe 1994; Kraus 2002). Kraus and Aslan (1999) describe this cyclic hierarchy as the product of micro-scale (< 1 m thick, duration of days to months), meso-scale (> 1 m thick, 1–10^2 yr duration), macro-scale (> 10 m thick, 10^3–10^4 yr duration), and mega-scale (> 100 m, 10^5–10^7 yr duration) aggradational alluvial episodes. Micro-scale and meso-scale sedimentary cycles are attributed to autogenic processes such as individual flood events and lateral channel accretion, whereas macro-scale cyclicity is attributed to a combination of autogenic and allogenic processes such as channel avulsion, regional climate change, and neotectonics (Kraus and Aslan 1999). Mega-scale alluvial cyclicity is often regarded as the product of allogenic processes such as tectonic activity and variable climate (e.g., Allen 1978; Read and Dean 1982; Blakey and Gubitosa 1984; Posamentier and Allen 1993; Legarreta and Uliana 1998; Kraus 2002). Although there is general agreement in the literature that eustatic sea-level change may also influence mega-scale alluvial cyclicity (e.g., Wright and Marriott 1993; Shanley and McCabe 1994; Schwans 1995; Quirk 1996; Kraus and Aslan 1999), uncertainties often associated with the correlation of alluvial cycles with coeval marine units, along with the potential for destructive (or constructive) overprinting by tectonic or climatic events of varying frequency and magnitude, make confirmation of a eustatic-sea-level mechanism difficult (Posamentier and Weimer 1993; Shanley and McCabe 1994; Ethridge et al. 1998). Because of these ambiguities, convincing examples of alluvial cyclicity produced in response to eustatic sea-level change are uncommon in the pre-Quaternary sedimentary record.

This paper unravels the hierarchy of cyclic processes that resulted in accumulation of the latest Cretaceous through earliest Tertiary Aguja, Javelina, and Black Peaks formations within the Tornillo Basin of Big Bend National Park, west Texas. The most recent studies of the Cretaceous–Tertiary (K/T) transition within the Tornillo Basin provide biostratigraphic and magnetostratigraphic age constraints (see summaries in Lehman 1990, p. 362–363, and Lehman 1991, p. 14), documentation of the relationship between episodes of Laramide tectonism and styles of alluvial sediment fill (Lehman 1991), and reconstructions of climate history from paleosol descriptions (Lehman 1989; 1990). This study evaluates the K–T alluvial succession in the relatively continuous exposures along Dawson Creek (Figs. 1, 2). Detailed sedimentologic descriptions of the Dawson Creek outcrop, including the abundant paleosols in the succession, are used to: (1) document the hierarchy of alluvial cyclicity (*sensu* Kraus 1987; Kraus and Aslan 1999); (2) differentiate between composite autogenic and allogenic cyclic mechanisms; and (3) compare against published conceptual and empirical models of fluvial sequence stratigraphy. In particular, we apply one-dimensional analysis of alluvial stacking patterns to evaluate whether eustatic sea-level change may account for mega-scale alluvial cyclicity.

Stratigraphic Overview and Paleogeography

The Tornillo Basin spans the border of west Texas and northern Mexico, and occurs along what was, during latest Cretaceous and earliest Tertiary time, the tectonically active southwestern margin of the North American Western Interior Seaway (WIS) (Lehman 1991). Although bounded on the west and east by the Chihuahua Tectonic Belt and the Marathon Uplift, the basin maintained a hydrologic connection with the WIS (Kauffman 1984; Lillegraven and Ostresh 1990; Lehman 1991). The Tornillo Basin is highly asymmetric, with the axis of subsidence and associated thickest sedimentary accumulations located in the southeastern part of the basin (Fig. 1; Lehman 1986). The Dawson Creek section is situated approximately 50 km west of the basin axis (Figs. 1, 2). Upper Cretaceous (upper Campanian to Maastrichtian) and lower Paleocene (Danian) sedimentary fill is entirely fluvial, and was deposited during an episode of tectonism within the Chihuahua Fold and Thrust Belt (Lehman 1991).

Outcrop exposures along Dawson Creek are dominated by overbank mudrocks (66% of decompacted thickness) that include abundant and well-developed paleosols (Figs. 3, 4). The Dawson Creek section has the best

JOURNAL OF SEDIMENTARY RESEARCH, VOL. 74, NO. 3, MAY, 2004, P. 391–404
 1527-1404/04/074-391/$03.00

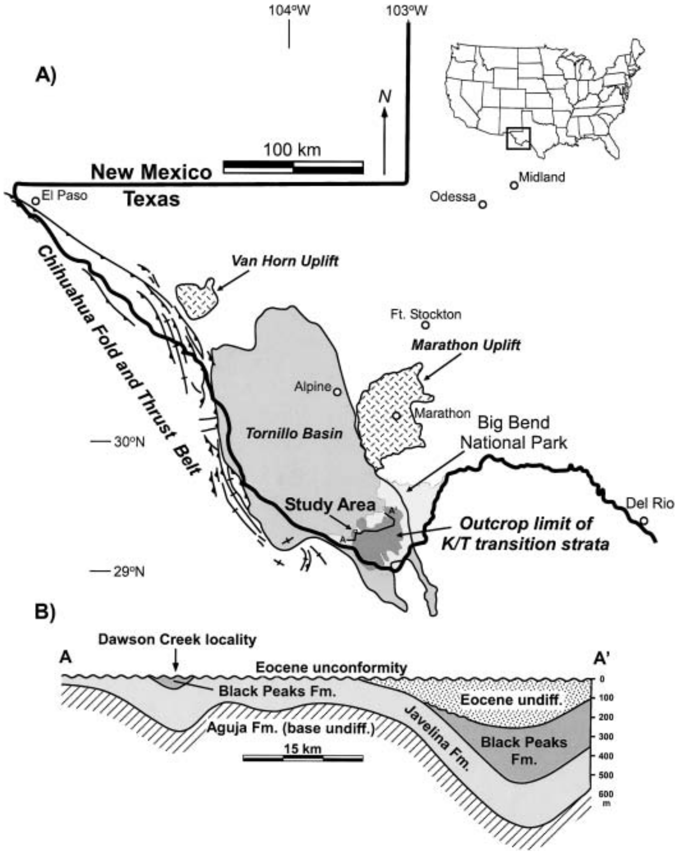

FIG. 1.—**A)** Map illustrating position of study area within the Tornillo Basin, and the distribution of other major Laramide structural features (modified from Lehman 1991). **B)** Diagrammatic cross section through the southeastern axis of the Tornillo Basin. Outcrop exposures along Dawson Creek are located approximately 50 km west of the basin axis (modified from Lehman 1986).

age control of any K–T exposures in the Tornillo Basin, having been dated by previous vertebrate biostratigraphic and magnetostratigraphic studies (Wilson 1970; Schiebout 1974; Rapp et al. 1983; Lehman 1985a; Standhardt 1986; and Runkel 1988 as cited in Lehman 1989, 1990, and 1991). The Aguja and Javelina formations occur within the Upper Cretaceous Judithian, Edmontonian, and Lancian North American Land-Mammal Ages, whereas the Black Peaks Formation is of Paleocene Puercan age (Fig. 5). Contacts between the Aguja, Javelina and Black Peaks formations are all conformable (Lehman 1985a), and all land-mammal stages and polarity zones are preserved within the study interval (Lehman 1990). This indicates that intraformational unconformity surfaces characterized by significant truncation are apparently lacking. No incisement surfaces having significant erosional relief were observed within the study interval. The K–T boundary is also conformable (Lehman 1990), and has previously been identified by Lehman (1989) as approximately coincident with the Javelina–Black Peaks contact (Fig. 5). The age of the study interval base is not known with certainty but includes the Upper Shale Member of the Aguja Formation. The presence of the *Kritosaurus* dinosaur assemblage in the lower part of the Upper Shale Member indicates a late Campanian age; fragmentary dinosaur remains within the upper portion of the Upper Shale Member do not exclude the possibility of an early Maastrichtian age (Lehman 1985a). The study interval extends from polarity Chron C31R, in the upper part of the Aguja Formation, to at least Chron C29N, near the base of the Black Peaks Formation (Lehman 1991) (Fig. 5).

METHODS

Data collected during outcrop description includes stratal thickness, grain size, mechanical and biological sedimentary structures, lithostratigraphic boundaries, and the stratigraphic occurrence of paleosol tops (Figs. 3, 4). Values of apparent thickness measured in the field were corrected to true vertical thickness by accounting for both southwestward structural dip (ranging from 14° to 36°) and outcrop surface slope angle (varying from 0° to 90°). Fluvial facies designations, appearing adjacent to the measured section presented in Figure 3, follow the classification scheme of Miall (1978), and are interpreted to occur within either an alluvial channel or an

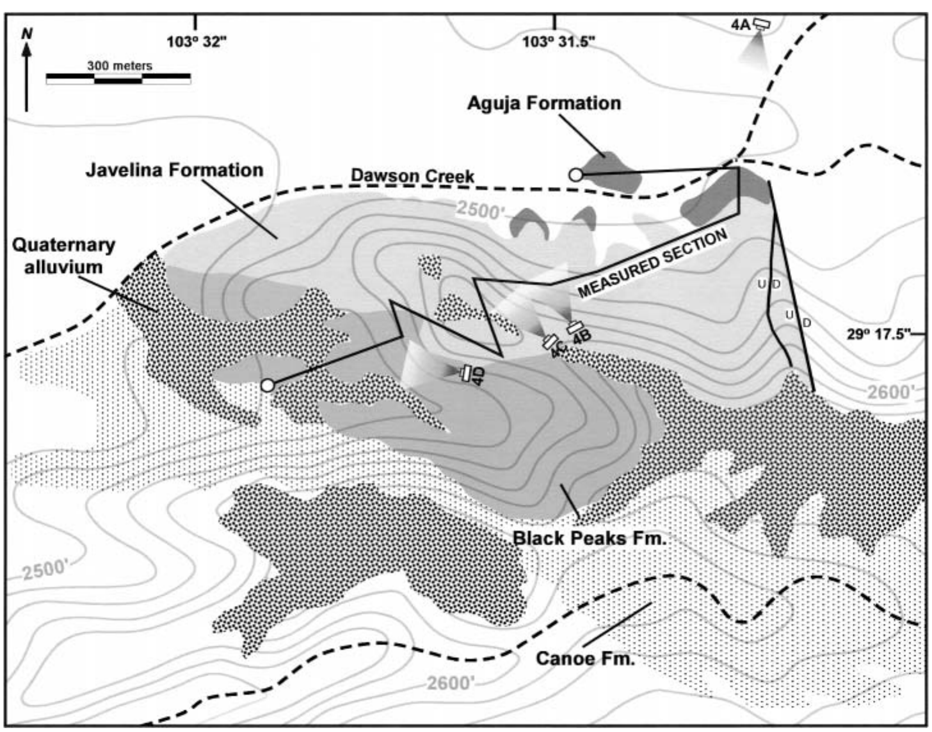

FIG. 2.—Topographic and geologic map of the Dawson Creek study area, Big Bend National Park, Brewster County, Texas (geologic map adapted from Lehman 1990). The surface trace of the measured section presented in Figure 3 is highlighted, as are the locations and orientations from which photopanoramas A–D (provided in Fig. 4) were taken.

overbank facies association (Tables 1, 2). During the course of field description, high-resolution digital photographs of the outcrop exposure were compiled into a series of photomosaics on a laptop computer and labeled with stratal surfaces and paleosol tops (compare Figs. 2, 3, and 4).

As the outcrop section was measured, paleosols were staked and numbered, labeled with survey tape, and described in detail. Paleosols were identified as having pedogenic features with systematic depth variations, and abrupt upper profile boundaries and gradational lower solum boundaries. Each paleosol horizon was described for thickness, boundary conditions, texture, structure, root traces, carbonate accumulation, reaction to hydrochloric acid, slickensides, and Munsell color, including redoximorphic features (Soil Survey Division Staff 1993; Retallack 2001). Genetic horizon symbols were assigned accordingly (Soil Survey Division Staff 1993), and from these, equivalent diagnostic horizons and modern soil orders were classified (Table 2, Fig. 6). The criteria used in assigning indices for paleosol maturity and drainage are summarized in Table 3.

The Dawson Creek interval was interpreted via ‘‘stacking-pattern analysis,’’ a technique that has been used by marine carbonate stratigraphers to decipher cyclic stratal hierarchies and their associated composite mechanisms within one-dimensional outcrop successions (see the *Introduction* to Lehrmann and Goldhammer 1999, p. 187–188). The stacking-pattern technique may similarly assist in the recognition and interpretation of long-period, allogenic processes within thick, relatively conformable alluvial successions that are dominated by overbank mudrock. In this study, thickness and grain size of fluvial aggradational cycles (FACs; see description in following section) were plotted graphically as the cumulative deviation from mean values, and compared with trends of changing facies proportion and paleosol maturity and paleosol drainage (Fig. 7). The procedures for the construction of cumulative deviation plots and the utility and potential shortcomings of cummulative deviation plots for cyclostratigraphic analysis are thoroughly discussed by Sadler et al. (1993), Drummond and Wilkinson (1993), and Lehrmann and Goldhammer (1999). To determine the cumulative deviation of grain size, the following numerical values were assigned to the standard Udden–Wentworth grain-size classes: 1 = mud, 2 = very fine sand, 3 = fine sand, 4 = medium sand, 5 = coarse sand, 6 = very coarse sand, 7 = gravel. From these, a median value was graphically determined from the detailed field measured section for each FAC. The median grain-size values for the total population of FACs were subsequently averaged (average grain size = 1.7), and the average value, along with the individual median grain-size values for each FAC, were used in the calculation of cumulative deviation from median grain size for the succession of FACs. It is these latter grain-size values that are plotted in Figure 7. Cumulative deviation from mean FAC thickness was calculated and plotted in a manner similar to that of grain size using an average decompacted FAC thickness of 5.9 m. The Dawson Creek section was decompacted using the algorithms of Sheldon and Retallack (2001); algorithm constants used in the decompaction of paleosols having diagnostic subsurface horizons (P_i, P_v, P_a), rooted overbank mudstone lacking diagnostic subsurface horizons (P_e), and alluvial sand are drawn from Table 1 of Sheldon and Retallack (2001) (compare with Tables 1 and 2 of this paper). The base of the study interval is estimated to have been buried beneath approximately 1500–2100 m of Late Cretaceous to Early Tertiary strata, and an unknown thickness of Miocene to Pleistocene strata (COSUNA 1983). Because of uncertainty in the actual burial depth of the Dawson Creek section base, a midpoint minimum burial depth of ~1800 m was used in the decompaction calculations.

Although a potentially useful tool for interpretation, the stacking-pattern technique described in the preceding paragraph has potential problems when applied to alluvial successions. First, intraformational surfaces of incisement, if present, strip FACs from the sedimentary record. In such instances, evidence of accommodation change is erroneously omitted and stacking pattern results are in all likelihood rendered meaningless. Although surfaces of significant incisement are not thought to exist in the Dawson Creek interval, they likely do exist in many, if not most, alluvial successions. Second, care must be taken to consistently (and accurately) identify the bases and tops of FACs. This may be difficult in amalgamated channel sands where FAC boundaries are ambiguous. Sand-body amalgamation, therefore, may cause an inaccurate estimation of FAC thickness and misrepresentation of associated accommodation trends. Interpretations derived from FACs in amalgamated channel sands are strengthened if similar thickness trends are observed in intercalated FACs composed exclusively of overbank mudrock. FAC boundaries within paleosol-bearing overbank mudrock successions are identified unambiguously. In the case of the Dawson Creek succession, FAC thickness trends in amalgamated channel sands are corroborated by similar thickness trends in interbedded FACs composed exclusively of overbank mudrock (Fig. 3). Finally, the destructive (or constructive) interference of long-period allogenic accommodation cycles (e.g., tectonic, climatic, eustatic) and shorter-period autogenic processes (e.g., random variations in flood frequency and magnitude, avulsion frequency, proximity to sediment source), may obscure, or destroy, accommodation trends (*sensu* Heller and Paola 1996). In the Dawson Creek succession, we feel that trends of FAC thickness, lithologic proportions, and grain size discriminate between allogenic and autogenic processes and demonstrate the utility of the stacking-pattern technique.

Cyclic Hierarchy

Paleosol-bearing alluvial successions commonly contain a hierarchy of cyclic stratal units (Beerbower 1964; Allen 1978; Bridge 1984; Kraus 1987; Kraus and Aslan 1999; Kraus 1999; Kraus 2002). Meter-scale depositional cycles (*simple pedofacies sequences* of Kraus 1987) occur within decameter-scale depositional cycles (*compound pedofacies sequences* of Kraus 1987). Both meter- and decameter-scale cycles are paleosol-capped, coarsening- or fining-upward alluvial successions (e.g., Kraus 1987; McCarthy and Plint 1998). Hectometer-scale cycles (*pedofacies megasequences* of Kraus 1987; *alluvial sequences* of Wright and Marriott 1993, and Shanley and McCabe 1994) are characterized by both a distinctive change in soil maturity (e.g., Kraus 1987; Plint et al. 2001) and sandstone/mudstone ratio. From base to top, hectometer-scale cycles display an initial upsection decrease, followed by an increase in soil maturity that coincides with a change in fluvial style from braided (or meandering), multi-story sandbodies that have a limited volume of associated overbank mudrocks, to meandering, single-story sandbodies encased within abundant overbank mudrocks (e.g., Blakey and Gubitosa 1984; Wright and Marriott 1993; Schwans 1995; Cant 1998; Legarreta and Uliana 1998; Martinsen et al. 1999).

The K–T section exposed along Dawson Creek is composed of a similar hierarchy of meter-scale FACs, decameter-scale fluvial aggradational cycle sets (FAC sets), and hectometer-scale fluvial sequences (Fig. 3). A total of 49 thin (average measured thickness = 5.0 m, average decompacted thickness = 5.9 m), generally fining-upward FACs occur in the study interval (Figs. 3, 4). FACs have an abrupt basal contact overlain by sandstone or mudstone that either gradationally transitions into a paleosol or is abruptly overlain by the succeeding FAC without an intervening paleosol. Forty-three of the 49 FACs are gradationally overlain by a paleosol (Figs. 3, 4, 6).

Trends of changing facies proportion, grain size, and paleosol maturity suggest that FACs stack into six FAC sets that range in thickness from 22 m to 68 m (Figs. 3, 7). Between 4 and 12 (average = 8) FACs constitute each FAC set. The bases of FAC sets are dominated by single-story to double-story sandstone or gravelly sandstone bodies and interbedded laterally discontinuous paleosols that grade into paleosol-rich overbank mudrocks at their top. From base to top within each FAC set, paleosols display either a gradual increase in soil maturity and drainage (e.g., FAC sets 3, 5) or a somewhat asymmetrical pattern of increasing and decreasing maturity and drainage (e.g., FAC sets 2, 4) (Fig. 3).

Long-period trends of FAC thickness, lithologic proportions, and paleo-

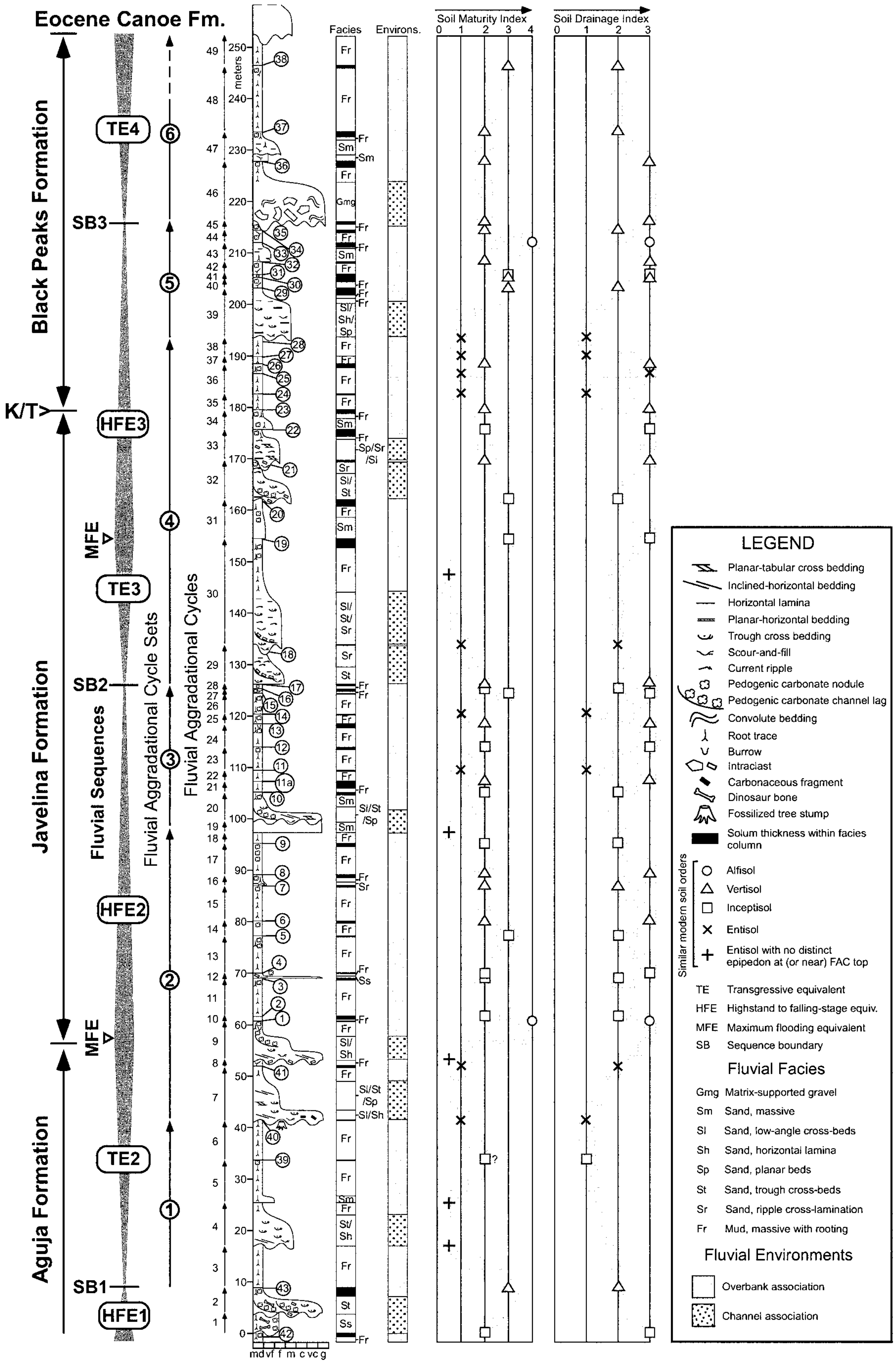

Eocene Canoe Fm.
Black Peaks Formation
Javelina Formation
Aguja Formation
K/T
TE4
SB3
HFE3
MFE
TE3
SB2
HFE2
MFE
TE2
SB1
HFE1
Fluvial Sequences
Fluvial Aggradational Cycle Sets
Fluvial Aggradational Cycles
meters
md vf f m c vc g
Facies
Environs.
Soil Maturity Index
Soil Drainage Index
LEGEND
Planar-tabular cross bedding
Inclined-horizontal bedding
Horizontal lamina
Planar-horizontal bedding
Trough cross bedding
Scour-and-fill
Current ripple
Pedogenic carbonate nodule
Pedogenic carbonate channel lag
Convolute bedding
Root trace
Burrow
Intraclast
Carbonaceous fragment
Dinosaur bone
Fossilized tree stump
Solum thickness within facies column
Similar modern soil orders
Alfisol
Vertisol
Inceptisol
Entisol
Entisol with no distinct epipedon at (or near) FAC top
TE Transgressive equivalent
HFE Highstand to falling-stage equiv.
MFE Maximum flooding equivalent
SB Sequence boundary
Fluvial Facies
Gmg Matrix-supported gravel
Sm Sand, massive
Sl Sand, low-angle cross-beds
Sh Sand, horizontal lamina
Sp Sand, planar beds
St Sand, trough cross-beds
Sr Sand, ripple cross-lamination
Fr Mud, massive with rooting
Fluvial Environments
Overbank association
Channel association

TABLE 1.—*Channel-association facies and criteria for recognition. All facies occur within a complex of thick (5–20 m) tabular sandstone bedsets that extend at least hundreds of meters laterally.*

Facies	Features	Interpretation
Ss/Sl	Graded fine to coarse sand with granule to gravel lag along inclined or horizontal reactivation surfaces. Gravel lag is often composed of reworked pedogenic carbonate nodules and to a lesser extent carbonaceous and bone material	Upper-flow-regime channel scour.
Sh	Fine to medium sandstone with parting lineation along inclined and planar-horizontal laminae.	Upper-flow-regime channel fill.
St	Trough cross-bedded fine to medium sandstone; reworked pedogenic carbonate nodules and to a lesser extent carbonaceous and bone material along reactivation surfaces.	Lower-flow-regime 3-D dunes as channel fill.
Sp	Fine to medium sandstone with planar-tabular cross stratification.	Lower-flow-regime 2-D dunes as channel fill.
Sr	Very fine to fine rippled sandstone. Root casts rare to common.	Lower-flow-regime current ripples as channel fill.
Sm	Very fine to medium massive sandstone. Root casts rare to common.	Channel-filling debris, and/or primary bedform destruction by secondary biological activity. *Bedforms may possibly be present but are not resolvable due to poor outcrop preservation.*
Gmg	Matrix-supported mudstone clasts (0.1 to 1 m in longest dimension). Clasts are composed of Fr and P facies (see Table 2). Massive and non-sorted.	Channel-filling debris flow derived from channel-bank slump.

sol maturity and drainage indicate that the study interval is composed of two complete and two partial fluvial sequences (Figs. 3, 7). Sequences 2 and 3 are both characterized by an upsection asymmetric increase and decrease in FAC thickness, and a corresponding upsection decrease in channel-association fluvial facies (Figs. 3, 7). Paleosols are increasingly well-drained and more mature from base to top in sequences 2 and 3 (Fig. 3). Paleosols in the lower half of sequences 2 and 3 are most similar to modern Entisols, whereas paleosols in the upper half are most similar to modern Inceptisols, Vertisols, and Alfisols. Paleosols at or slightly below sequence boundaries 1, 2, and 3 are among the most mature observed in the entire study interval (Fig. 3). Only the uppermost 10 m of sequence 1 is exposed in outcrop, and it is characterized by mature, well-drained paleosols and tabular channel sandstone bodies that contain reworked pedogenic carbonate nodules and dinosaur bones (Fig. 3). Only the lowermost 37 m of sequence 4 is exposed in outcrop, and it is characterized by thick, channel-filling sandstone and debris at the base that are overlain by overbank mudrocks and associated poorly-drained paleosols of intermediate maturity (Fig. 3). The channel-filling debris is thought to have been derived from a cutbank slump.

Sequences are subdivided into systems-tract equivalents based upon vertical changes in FAC thickness, depositional environments, and paleosol maturity and drainage (Figs. 3, 7). Transgressive-equivalent (TE) strata are characterized by upward-thickening FACs that contain the highest proportion of channel-association deposits and least mature and most poorly-drained paleosols. Overlying highstand- to falling-stage-equivalent (HFE) strata are dominated by upward-thinning FACs that consist largely of overbank mudrocks and associated mature and well-drained paleosols.

DISCUSSION

Cyclic Mechanisms

The nature of FACs and FAC sets suggests depositional mechanisms consistent with the autogenic models for similar-scale fluvial cycles proposed by Bridge (1984), Kraus (1987), and Kraus and Aslan (1993, 1999). FACs are interpreted to record individual episodes of channel avulsion and ensuing, prolonged periods of channel stability (*sensu* Kraus and Aslan 1993). During avulsion episodes, sedimentation rates across the floodplain were relatively high, and subsequently, horizon development in paleosols was weak. As a result, all mudrock and some sandstone bodies in the lower parts of Dawson Creek FACs have abundant root casts but no horizon development in paleosols (Fig. 6F, G, H). Channel stabilization following avulsion reduced the rates of sediment accumulation on the floodplain and allowed strong horizon development in paleosols. Forty-one Dawson Creek FACs have strongly developed paleosols at their top (Figs. 3, 6A, B, C).

FAC sets are interpreted to have been produced by successive episodes of avulsion such that the channel drifted away from, and back to, a reference position in the alluvial valley (*sensu* Kraus 1987). The upward change within FAC sets from sand- to mud-dominated textures, and the corresponding variations in paleosol maturity and drainage, may reflect a progressive change in the location of the overbank sediment source (Figs. 3, 7). Channel migration away from the outcrop locality caused a reduction in grain size and in rate and frequency of sediment accumulation on the floodplain, whereas channel migration toward the outcrop locality resulted in an increase in grain size and rate and frequency of sediment accumulation on the floodplain (*sensu* Bown and Kraus 1987). An avulsive channel drift mechanism for FAC sets should, therefore, also be expressed in trends of FAC thickness; progressive channel migration away from the outcrop locality should have resulted in an upward thinning and fining of FACs, and vice versa. Although a positive correlation does exist between grain size and FAC thickness for the Dawson Creek succession (particularly within FAC sets 4–6), the trend appears to be muted by the longer-period thickening and thinning trend that coincides with hectometer-scale fluvial sequences (Fig. 7).

Hectometer-scale fluvial sequences have been attributed to allogenic mechanisms such as tectonics (uplift and/or subsidence), a change in regional or global climate, or fluctuations in eustatic sea level (e.g., Posamentier and Allen 1993; Schumm 1993; Shanley and McCabe 1994; Schwans 1995; Kraus and Aslan 1999). Most previous studies generally consider fluvial sequences dominated by overbank mudrocks, similar to those observed along Dawson Creek, to be the result of various tectonic mechanisms (Kraus and Aslan 1999). Eustatic sea-level change may also cause fluvial cyclicity (e.g., Aslan and Autin 1999; Blum and Tornqvist 2000); however, relatively few convincing examples from fully fluvial successions exist in the pre-Quaternary record (e.g., Rogers 1998; Plint et al. 2001). The lack of examples may be because most successions available

←

FIG. 3.—Dawson Creek measured section, presented at non-decompacted thickness (compare with Figs. 2, 4). Labeled to the left of the graphical measured section is the position of fluvial aggradational cycles (FACs, numbered 1–49 and highlighted with small arrows), fluvial aggradational cycle sets (FAC sets, circled numbers 1–6 and highlighted with larger arrows), fluvial sequences including sequence stratigraphic components (sequence 1 occurs beneath SB1, sequence 2 beneath SB2, etc.), and lithostratigraphic names including placement of the Cretaceous–Tertiary (K–T) boundary. Labeled to the right of the measured section are the positions of paleosols (circled numbers, 1–43), fluvial facies designations (after Miall 1978) and their interpreted environmental associations (explanation in Tables 1, 2), and indices for soil maturity and drainage (explanation within Table 3). Value trends of soil maturity and drainage are shaded gray. Sequence boundaries (SB1–3) occur at the inflections between thinning (highstand- to falling stage-equivalent, HFE1–3) and thickening (transgressive-equivalent, TE2–4) FACs. Highstand- to falling stage-equivalent FACs are overlain by well-drained, mature paleosols, whereas transgressive-equivalent FACs are overlain by more poorly-drained, immature paleosols. The maximum flooding equivalent (MFE) for sequences 2 and 3 is placed at the inflection between thickening- and thinning-upward FACs and their corresponding transition from poorly-drained, immature paleosols to well-drained, mature paleosols.

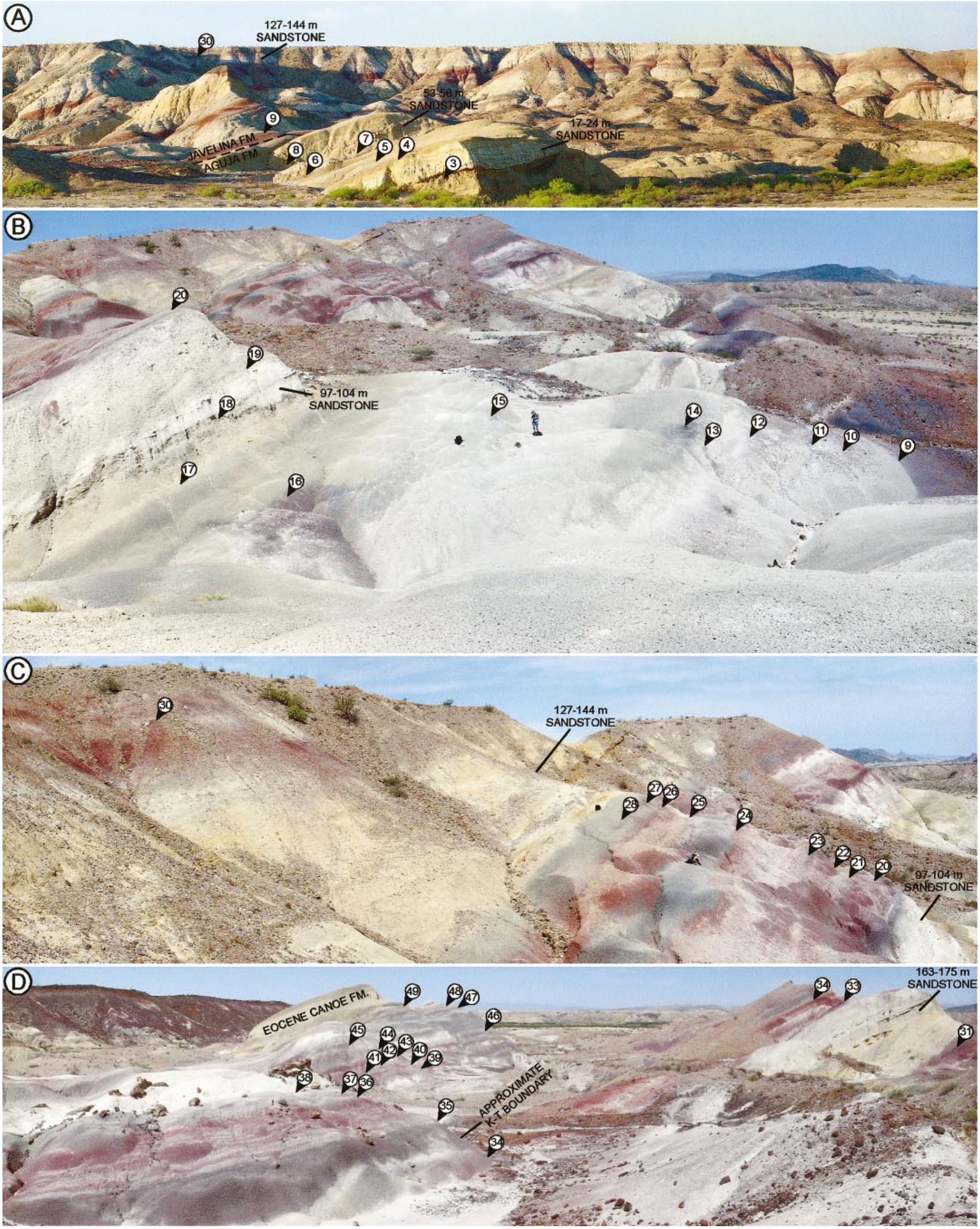

FIG. 4.—**A–D)** Photopanoramas of the outcrop section labeled with FAC tops (circled numbers), major sandstone complexes, and the K–T boundary. Compare with Figures 2 and 3.

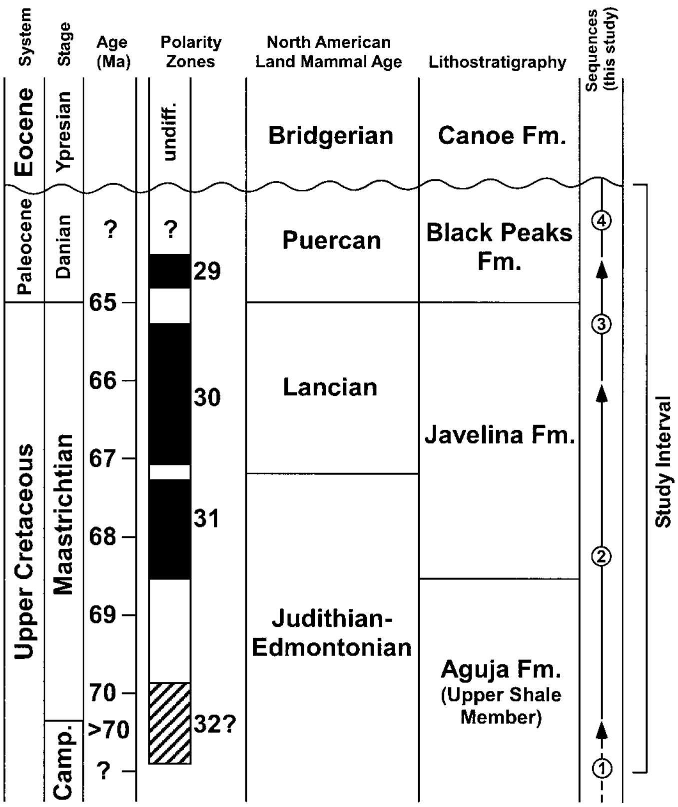

FIG. 5.—Chronostratigraphic correlation chart (compiled from Lehman 1990; Lillegraven and Ostresh 1990; Lehman 1991; Gradstein et al. 1994) annotated with fluvial sequences identified in this study.

for study were either deposited within hydrologically closed basins or accumulated in a position too distant from the time-equivalent shoreline for the effects of eustatic sea-level change to be expressed. Additionally, outcrop or subsurface datasets where fluvial deposits and their marine equivalents can be convincingly correlated are extremely rare (e.g., Plint et al. 2001).

Within the Tornillo Basin, Lehman (1991) suggests that a single pulse of tectonism accounts for an increase in sedimentation rate and the associated introduction of coarser-grained, extrabasinal sedimentary detritus during deposition of the Maastrichtian Javelina Formation. Systematic variations in FAC thickness, facies proportions, and paleosol maturity and drainage, however, indicate that higher-frequency accommodation cycles were superimposed upon the Javelina tectonic pulse and resulted in the accumulation of alluvial depositional sequences (Figs. 3, 7). Although depositional sequences may be the product of fluctuating subsidence rates, they appear to correlate more closely with known episodes of eustatic sea-level change. On the basis of detailed biostratigraphic and magnetostratigraphic correlation, Kauffman (1977, 1984) identifies ten third-order epicontinental marine cyclothems (TR 1–10) in the Cretaceous of the WIS. Continental-scale correlations between cratonic basins of the WIS suggest that TR1–10 may have been eustatically derived, or at least eustatically influenced (Caldwell et al. 1993). The TR8 regression is age-equivalent to the Upper Shale Member of the Aguja Formation (Stevens and Stevens 1989; compare Lehman 1990, Lillegraven and Ostresh 1990, Lehman 1991, and Robinson-Roberts and Kirschbaum 1995) and therefore coincides with the uppermost portion of sequence 1 (Fig. 5). TR9 and TR10 are approximately age-equivalent with sequences 2 and 3 of the uppermost part of the Upper Shale Member and the overlying Javelina and Black Peaks formations (Fig. 5). A similar chronology of Late Campanian through Maastrichtian transgressive–regressive depositional events has also been recognized by Sugarman et al. (1995) and Miller et al. (1999) in the coastal plain of New Jersey, U.S.A., and attributed to a eustatic mechanism. The lower part of sequence 4 coincides with the Paleocene (earliest Danian) major marine transgression documented by Davidoff and Yancey (1993) in the Brazos River Valley of south-central Texas.

Critical to the interpretation of eustatic sea level change as the cause of

TABLE 2.—*Overbank-association facies and criteria for recognition. All sandstone facies (Sr, Sm, Ss) occur at thin ($\ll$ 5 m) tabular sandstone bed(s) that extend less than hundreds of meters laterally. Summary of diagnostic attributes for the various soil horizons is provided at the bottom of the table.*

Facies	Features	Interpretation
Fr (P_e)	Paleosol. Typically A(g)–C(g) or A–Bg profiles with no diagnostic subsurface horizons. Ochric epipedon is rooted and exhibits weak soil structure. Lower color values and chromas in comparison with other interpreted soil orders reflect wet conditions and aquic moisture regime.	Similar to modern Entisol.
(P_i)	Paleosol. Typically A–Bw or A–Bk profiles with Ochric epipedons over Cambic or Calcic subsurface horizons. Cambic has slightly higher chromas (reddening) than underlying parent material, and > 50% of the original parent material transformed to soil structure. No vertic properties or Argillic horizons observed.	Similar to modern Inceptisol.
(P_v)	Paleosol. Has > 30% clay and slickensides or wedge-shaped aggregates in the upper 50 cm of soil profile. Most commonly A–Bss–Bk profiles. Surface horizons are Ochric and subsurface horizons either Cambic or Calcic.	Similar to modern Vertisol.
(P_a)	Paleosol. A–E–Bt–Bk profiles with Ochric epipedons over Argillics and Calcics. Argillic horizon has > 20% increase in clay compared to overlying eluvial horizons and evidence of illuviation via clay skins.	Similar to modern Alfisol.
Sr (weakly developed P_e)	Very fine rippled to millimeter-laminated sandstone with common root casts.	Lower-flow-regime current ripples as overland sand sheet or crevasse splay.
Sm (weakly developed P_e)	Very fine massive sandstone with common root casts.	Stabilized overland sand sheet or crevasse splay.
Ss	Graded fine to coarse sand with granule or pebble lag along scoured base.	Proximal crevasse splay or upper-flow-regime overland sand sheet.
A-	When preserved, has darker colors than other horizons. Structure is fine to medium, subangular blocky to blocky. Root traces are rare to common.	
Bw-	Has brighter colors than the underlying parent material. Structure is medium to coarse, subangular blocky to blocky, or prismatic. Root traces are rare to common.	
Bg-	Colors range from gray to bluish green. Medium to coarse, subangular blocky to blocky structure, and rare to common root traces.	
Bss-	Fine to coarse, wedge-shaped aggregates with few to many slickensides. Rare to few root traces. May contain pedogenic carbonate nodules (Bssk). Colors range from yellow to brown to red. Root traces are rare to few.	
Bt-	Has more clay than the overlying A and/or A and E horizons. Structure is medium to coarse blocky or prismatic. Colors are brown to red to purple. Root races are rare to few.	
Bk-	Contains 1 to 15% pedogenic carbonate nodules that are typically pitted, white to grayish brown to brown, and 0.5 to 4 cm in diameter. Structure is medium to coarse blocky or prismatic. Root traces are rare to few. (Calcic horizons are Stage II in development, and have > 5% pedogenic carbonate nodules with > 15% estimated total carbonate content. The common occurrence of paleosols with Calcic horizons is suggestive of a subhumid to perhaps semiarid climate.)	

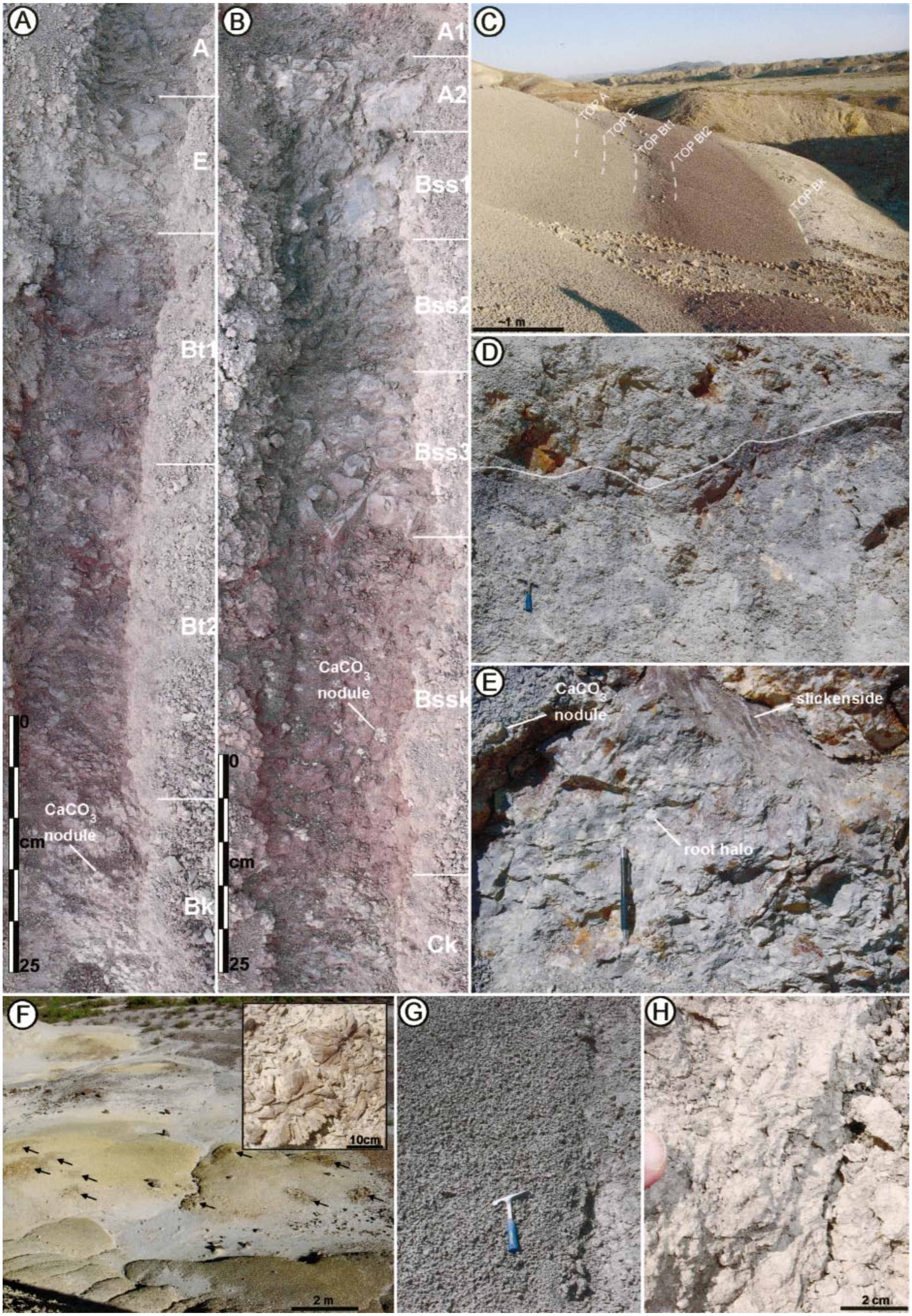
A
B
C
D
E
F
G
H
A
E
Bt1
Bt2
Bk
CaCO3 nodule
0
cm
25
A1
A2
Bss1
Bss2
Bss3
Bssk
Ck
CaCO3 nodule
0
cm
25
TOP A
TOP E
TOP Bt1
TOP Bt2
TOP Bk
~1 m
CaCO3 nodule
slickenside
root halo
10cm
2 m
2 cm

fluvial sequences is a determination of whether latest Cretaceous and earliest Tertiary shorelines were close enough to the study area to have influenced cyclic patterns of fluvial aggradation. On the basis of studies of the Mississippi River, Blum and Tornqvist (2000) suggest that the updip limit of fluvial onlap due to Quaternary sea-level rise extends at least 300–400 km landward of the shoreline for low-gradient, high-sediment-supply fluvial systems. Similarly, Aslan and Autin (1999) demonstrate a change in the alluvial style of the Mississippi River up to 300 km inland from the present coastline in response to a rapid rise in sea-level 5 to 10 ka before present. Perhaps a similar alluvial response is recorded within the Dawson Creek succession due to Late Cretaceous and early Tertiary sea level oscillations. Shanley and McCabe (1993) and Rogers (1998) in studies of Turonian through Campanian strata of Utah and Montana, U.S.A., corroborate this possibility by concluding that sea-level change may account for ''transgressive'' and ''highstand'' alluvial deposits from one hundred to several hundred kilometers inland from the equivalent coastline. The Late Cretaceous TR9–10 shorelines were within 25 to 200 km of the Dawson Creek section (Lillegraven and Ostresh 1990; Lehman 1991; Moran-Zenteno 1994; Robinson-Roberts and Kirschbaum 1995), and oscillated across the Parras and La Popa basins of northeastern Mexico where two, age-equivalent, hectometer-scale, transitional marine–nonmarine depositional sequences were deposited (Fig. 8) (Wolleben et al. 1970; McBride et al. 1974). The Paleocene (Danian, R10) shoreline was approximately 500 km from Dawson Creek (Fig. 8) (Davidoff and Yancey 1993). Because Late Cretaceous shorelines were always within 200 km of the study area, it is possible that third-order sea-level oscillations are recorded within the K–T succession of the Tornillo Basin.

Direct comparison of the K–T alluvial response with a Quaternary analog is, however, problematic. Although K–T alluvial systems in the vicinity of the Tornillo Basin are interpreted as low gradient and relatively high sediment load (Lehman 1991), the alluvial network most likely maintained significantly less capacity and higher gradient than that of the modern Mississippi River. The Nueces, Trinity, and Colorado rivers of the Texas Gulf Coastal Plain may serve as better modern analogs. These rivers are of higher gradient and lower capacity than the Mississippi River and are characterized by alluvial plains that onlap only between 40 and 90 km landward of the present coastline in response to Quaternary sea-level rise (Blum and Tornqvist 2000). Further complicating the comparison is that although the amplitude of sea-level change for the Late Cretaceous and Holocene are somewhat similar (i.e., $\sim$0–100 m for the Holocene versus $\sim$20–60 m for the Late Cretaceous), the period of sea-level change may vary by as much as two orders of magnitude (i.e., $\sim$10,000 years for the Holocene versus $\ll$ 1.0 Myr for the K–T transition) (Haq et al. 1988; Chappell et al. 1996; Miller et al. 1999). Earliest Paleocene sea-level rise also had an $\sim$1.0 Myr duration and $\sim$20–50 m amplitude (Haq et al. 1988).

From these comparisons, it seems unlikely that the low-capacity K–T alluvial systems could have attained equilibrium, and produced an aggradational record considerable distances inland from the equivalent coastline in response to the more rapid rates of sea-level rise characteristic of the Quaternary. It does seem possible, however, that an areally extensive, aggradational alluvial record could have been produced in response to the much longer-duration transgressive episodes that were likely characteristic of the Late Cretaceous. The much slower rate of Late Cretaceous sea-level rise inferred from Kauffman (1984) for T9 and T10 in the WIS may have provided ample time for the lower-capacity fluvial systems of the Tornillo Basin to establish (or approach) fluvial equilibrium through sediment aggradation. This may also have been the case for the earliest Paleocene transgression, but the $\sim$500 km distance to the equivalent transgressive shoreline casts doubt on this possibility.

TABLE 3.—*Paleosol maturity and drainage indices.*

	Rank	Features
Maturity[a]		
1	Very weakly developed	Weak mineral surface horizon (A); no subsurface horizon; massive to faint bedding; root traces.
2	Weakly developed	Mineral surface horizon (A); incipient subsurface Bk horizons with less than 5% carbonate nodules not qualifying as a Calcic diagnostic horizon.
3	Moderately developed	Mineral surface horizon (A); subsurface Bk horizon with more than 5% carbonate nodules qualifying as a Calcic diagnostic horizon.
4	Strongly developed	Mineral surface horizon (A) and E horizon; red or purple subsurface Bt horizon with sufficient clay enrichment to qualify as an Argillic diagnostic horizon.
Drainage[b]		
1	Poorly drained	Gray or blue-green surface and subsurface horizons.
2	Moderately drained	Yellow or brown subsurface horizons.
3	Well drained	Red or purple subsurface horizons.

[a] Modified from Retallack (2001) to fit key maturity properties in the study area.
[b] Based on general correlations between soil color and drainage where gray and blue-green indicate loss of iron from anaerobic conditions, yellow and brown indicate hydrated and oxidized iron, and red and purple indicate dehydrated and oxidized iron (see Soil Survey Division Staff 1993 and Richardson and Vespraskas 2001). Iron depletions along former root channels were not considered because their origin is likely from postburial gleying (Retallack 2001).

Sequence Stratigraphy

Conceptual models of alluvial sequence stratigraphy have been proposed by Wright and Marriott (1993), Shanley and McCabe (1994), Schwans (1995), Van Wagoner (1995), Retallack (1998), Kraus and Aslan (1999), and Boyd et al. (2000) and evaluated by empirical studies of Late Cretaceous transitional alluvial–marine strata in the WIS (e.g., Olsen et al. 1995, Aitken and Flint 1996, Rogers 1998, McCarthy and Plint 1998, McCarthy et al. 1999, and Plint et al. 2001). From these studies, an alluvial sequence stratigraphic model has evolved which suggests that hectometer-scale alluvial sequences often record the systematic adjustment of the fluvial system to rising and falling base level. Rapid base-level rise causes increasing accommodation and more frequent deposition of thick, flood-event deposits and associated poorly developed paleosols across a potentially poorly-drained, muddy floodplain. In more humid climates coastal-plain deposits may include lacustrine facies and coal (e.g., McCarthy et al. 1999, Plint et al. 2001), whereas in less humid climates alluvial deposits are dominated

←

FIG. 6.—Selected outcrop photographs of paleosols and associated features (compare with Fig. 3). **A)** Paleosol 33 (top of FAC 43) labeled with soil-horizon symbols and subordinate indicators. This paleosol is interpreted as similar to a modern Alfisol. The presence of a mineral surface horizon, A, and a well-developed, red Bt horizon indicates a maturity rank of 4 and a drainage rank of 3 (Table 3). **B)** Paleosol 30 (top of FAC 40) labeled with soil-horizon symbols and subordinate indicators. This paleosol is interpreted as similar to a modern Vertisol. The presence of a mineral A horizon, the lack of a subsurface Bt horizon, the presence of slickensides and other vertic features, and a Bk horizon having $>$ 5% carbonate nodules indicate a maturity rank of 3 (Table 3). The red color of the subsurface horizons yields a drainage rank of 3 (Table 3). **C)** Paleosol 1 (top of FAC 9) labeled with soil-horizon symbols and subordinate indicators. This paleosol provides an example of the typical appearance of unexcavated paleosol exposures. Paleosol 1 is interpreted as similar to a modern Alfisol. **D)** Gilgai surface of paleosol 43 (top of FAC 2) with an A–Bssk horizon sequence similar to a modern Vertisol. **E)** Well-developed slickenside, carbonate nodules, and root reduction haloes within the Bssk horizon of paleosol 43. **F)** Arrows indicate the location of recently exhumed fossil cycad stumps along an outcrop surface coincident with the upper part of paleosol 40 (FAC 6). Inset photograph provides a close-up view of an exhumed fossil cycad stump. Paleosol 40 is interpreted as similar to a modern Entisol. **G)** Mudrock overbank material beneath paleosol 24 (FAC 35). The massive structure of the mudrock, the lack of soil horizons, and the presence of abundant root casts indicate pedogenic development similar to a modern, poorly-drained Entisol. **H)** Closeup of deep root casts observed in the massive mudrock beneath paleosol 24 (FAC 35).

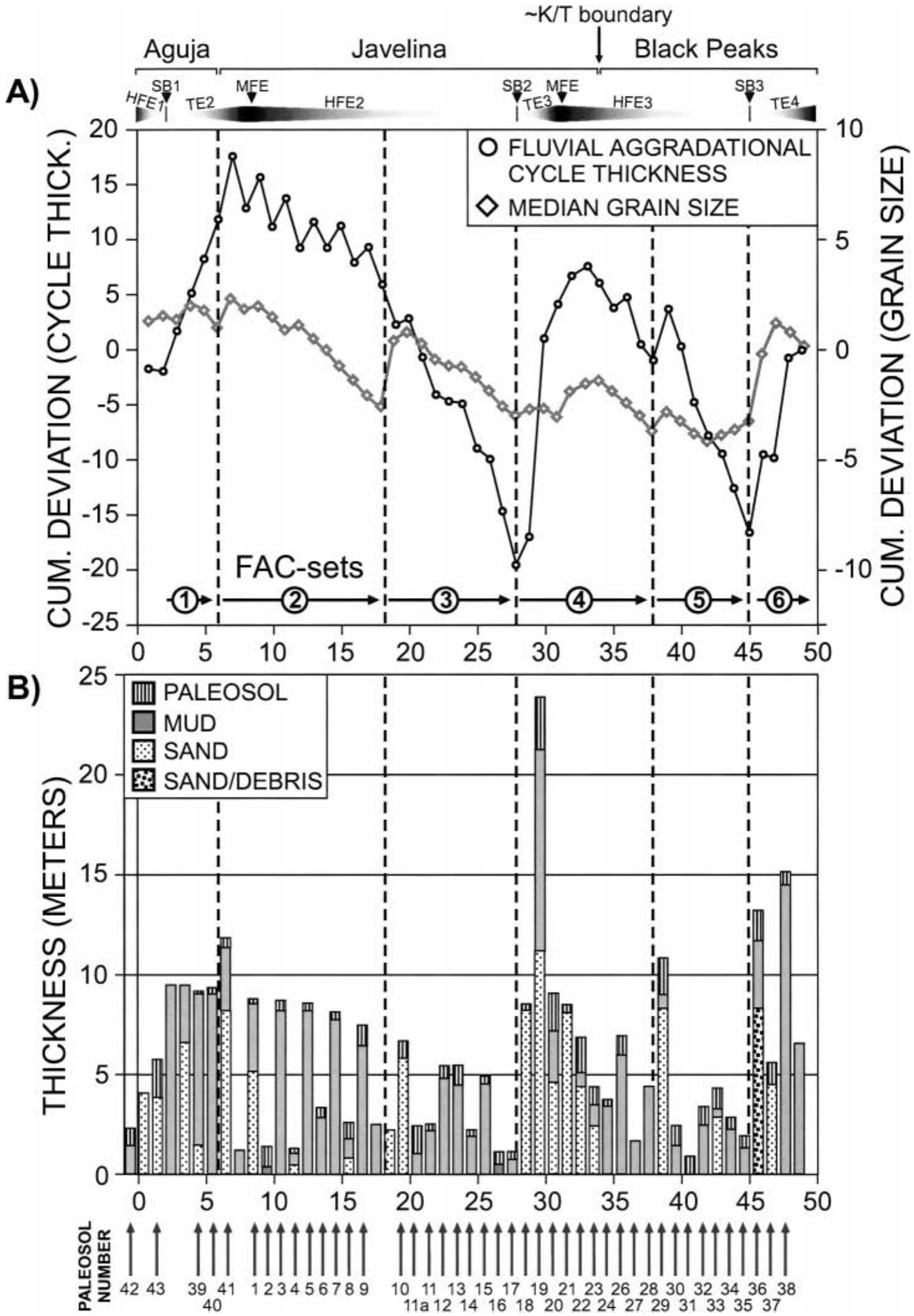

FIG. 7.—**A)** Cumulative deviation from mean-value plots for FAC decompacted thickness and median grain size. The *x* axis corresponds with FAC number (scaled 0–50). The left-hand *y* axis measures the cumulative deviation of individual FAC thickness values from the average thickness of all FACs (average FAC decompacted thickness = 5.9 m). The right-hand *y* axis measures the cumulative deviation of median grain size for individual FACs from the average of median grain-size values for all FACs (average = 1.7). Highlighted with dashed lines in the plot are FAC set boundaries (circled numbers 1–6), and above the plot are lithostratigraphic unit names, sequence boundaries (SB), and systems-tract equivalents (TE = transgressive-equivalent; HFE = highstand- to falling stage-equivalent). **B)** Histogram of FAC decompacted thickness and lithologic proportions at the same *x* axis scale as the cumulative deviation plots. Dashed lines highlight boundaries of FAC sets. The locations of numbered paleosols (from Fig. 3) are shown below the histogram.

by floodplain mudstone that commonly includes hydromorphic paleosols (e.g., Rogers 1998). Evidence of saturated conditions in both cases likely reflects both a rising water table and perhaps a shift towards a more humid climate in response to the approaching transgressive shoreline (*sensu* Rogers 1998).

As the rate of base-level rise decreases during late transgression and highstand, the associated reduction in accommodation causes a decrease in the frequency and thickness of flood-event deposits, and subsequently the development of increasingly mature paleosols. Depending on fluvial style and dominant overbank grain size, the resulting deposits may either include isolated anastomosed or meandering channel sandstone bodies encased in overbank mudstone or laterally amalgamated, tabular meander channel sandstone bodies (Cant 1998, Olsen et al. 1995, Holbrook 1996, Yoshida et al. 1996, and Rogers 1998 as discussed in Plint et al. 2001).

As base level slowly reaches a maximum and then recedes during the late highstand and ensuing falling stage, the rate of accommodation change is negligible and eventually negative, and increasingly well-drained, mature, oftentimes composite paleosols develop across a floodplain that is potentially reworked by laterally migrating channels. Channel incision and confinement during maximum lowstand causes both a lowering of the water table and a decrease in the frequency and magnitude of interfluve flood events. Fluvial incision during lowstand increases the likelihood that the most mature, well-drained paleosols develop atop the preceding interfluve highstand deposits (e.g., McCarthy and Plint 1998, McCarthy et al. 1999).

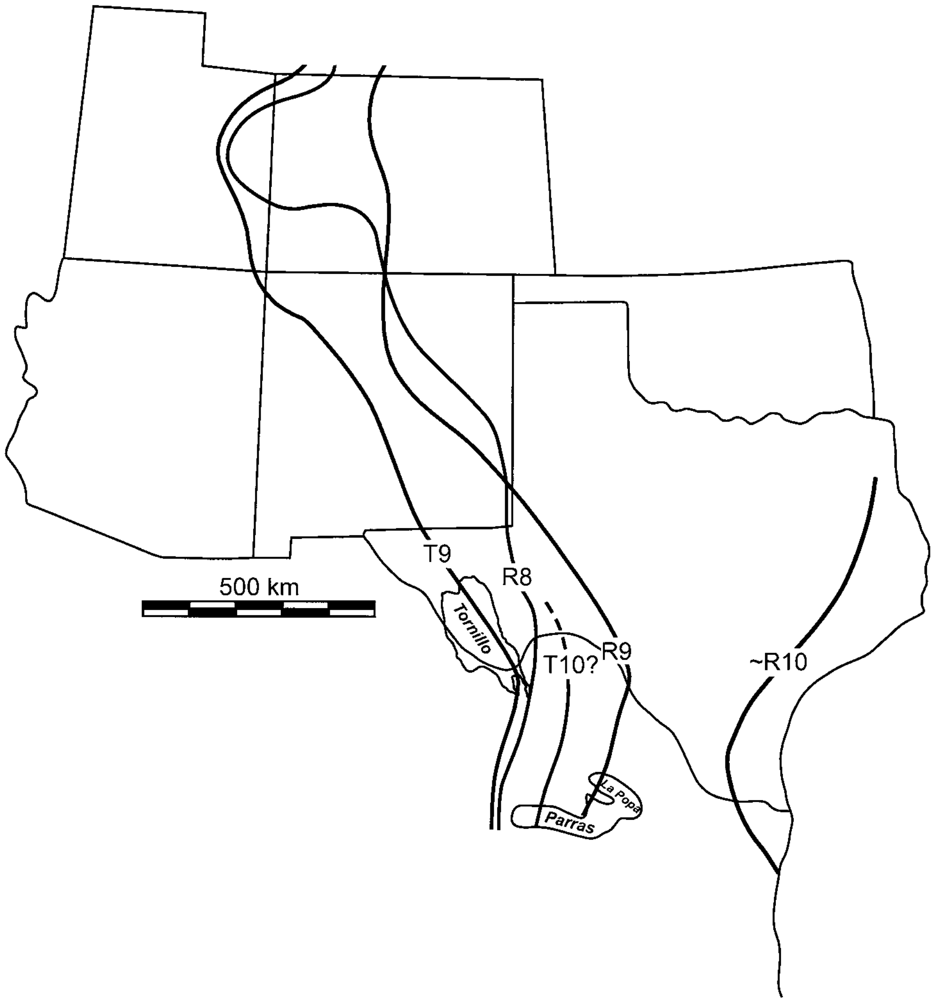

FIG. 8.—The location of Cretaceous (Campanian–Maastrichtian) and Paleocene (Danian) shorelines in the southwestern U.S.A. and Mexico (modified from Lehman 1985b; Lillegraven and Ostresh 1990; Davidoff and Yancey 1993; Moran-Zenteno 1994; Robinson-Roberts and Kirschbaum 1995). Outlines for the Tornillo, Parras, and La Popa basins are indicated. Designations of Cretaceous shorelines coincide with the numbered transgressive (T) and regressive (R) events of Kauffman (1977, 1984). The location of the latest Maastrichtian to Danian shoreline (R10) is estimated from Davidoff and Yancey (1993).

A subsequent rise in base level (and the water table) associated with the late lowstand to early transgressive phase may superimpose gleyed features onto the previously formed well-drained paleosols (Aitken and Flint 1996).

Our study corroborates many aspects of the alluvial sequence stratigraphic model described above (Fig. 9) and demonstrates that detailed description and interpretation of FAC-scale alluvial facies and pedofacies stacking patterns within relatively conformable, age-constrained, one-dimensional outcrop or subsurface core may assist in the identification of alluvial sequences and their stratal components (Figs. 3, 7). In some instances, analysis of alluvial stacking patterns may also assist in the correlation of depositional cycles between spatially discontinuous nonmarine and marine stratigraphic successions. At Dawson Creek, sequences coincide with long-period recurring trends of thickening and thinning FACs and their associated changes in fluvial facies and pedogenic features, and are thought to correlate with TR 8–10 of Kauffman (1977, 1984) (Figs. 3, 5, 7). Thickening and thinning FAC successions are interpreted to record third-order episodes of accelerating rise (transgressive-equivalent), decelerating rise (highstand-equivalent), and fall (latest highstand- and falling-stage-equivalent) in base level. The transgressive-equivalent part of each sequence is characterized by an upward decrease in the proportion of channel-association facies, and relatively few paleosols (Figs. 3, 7, 9). The overlying late highstand- to falling-stage-equivalent part has a higher proportion of overbank-association facies that include abundant paleosols (Figs. 3, 7, 9). Paleosols in each sequence are characterized by an irregular but generally steady increase in maturity and better drainage from base to top (asymmetric ''sawtooth pattern'' of Retallack, 1998). The irregular, cyclic variations within this sequence-scale trend coincide with FAC sets (Figs. 3, 9). Sequence boundaries are placed above the most mature and well-drained paleosols at the sharp inflection between thinning (highstand- to falling-stage-equivalent) and thickening (transgressive-equivalent) FACs (Figs. 3, 7, 9). Sequence boundaries 2 and 3 are placed directly above a succession of mature and well-drained paleosols and are overlain by FACs having the highest proportion of channel facies (Figs. 3, 7). Sequence boundary 1 lies above paleosol 43 (top of FAC 2) and is underlain by a tabular sand body (FACs 1 and 2) that contains abundant, reworked, pedogenic carbonate nodules (Fig. 3). FACs 1 and 2 beneath this boundary are interpreted to record late highstand- to falling stage-equivalent accommodation reduction and subsequent floodplain reworking by the lateral migration of meandering channel bodies.

Although late highstand- to falling stage-equivalent FACs thin dramatically toward sequence boundaries (Figs. 3, 7), no composite (i.e., superimposed) paleosols are observed at or near sequence boundaries. This is in contrast to the observations of McCarthy et al. (1999) and Plint et al. (2001) in the Cenomanian Dunvegan Formation of Alberta and British Columbia, Canada. Although no data currently exist to confidently determine why there is a lack of composite paleosols in the Dawson Creek section, there are at least several possibilities worth considering. First, the study interval may have experienced a higher long-term rate of accommodation gain throughout its entire history of accumulation, perhaps because of increased subsidence associated with the tectonic pulse of Lehman (1991) and con-

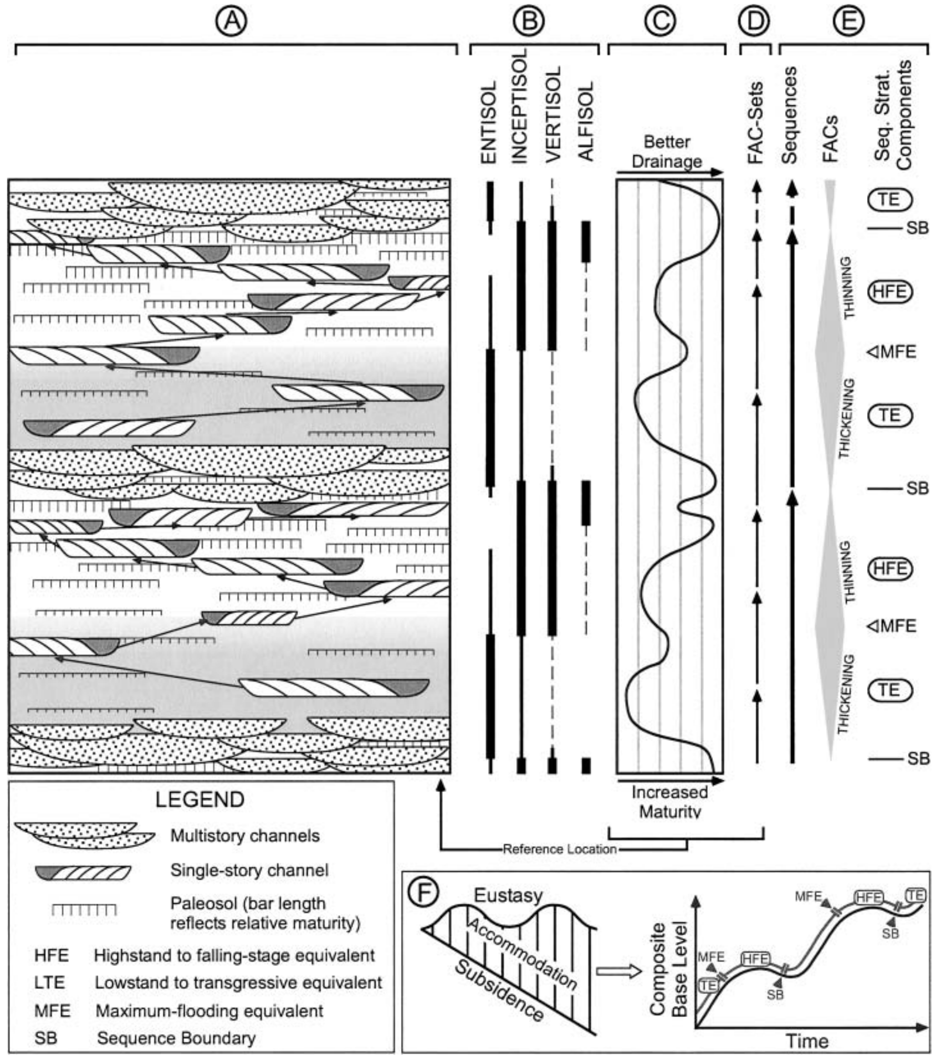

FIG. 9.—Conceptual diagram summarizing the Dawson Creek alluvial sequence stratigraphic model. **A)** Depiction of the stratigraphic succession. Arrows indicate a hypothetical scenario for channel avulsion and drift in an alluvial valley through time (*sensu* Bown and Kraus 1987). **B)** Vertical distribution and relative abundance of modern soil orders equivalent to Dawson Creek paleosols. Increasing bar width coincides with an increase in the relative abundance of paleosols. **C)** Paleosol maturity and drainage trends. Shorter-period cycles are interpreted to coincide with patterns of channel avulsion and associated drift in the alluvial valley over time relative to a fixed reference location (*sensu* Bown and Kraus 1987). Paleosols become more mature and better drained as the channel drifts away from the reference location. Longer-period cycles are interpreted to reflect episodes of rising and falling relative sea level (see discussion in Part E below). **D)** The vertical distribution of FAC sets. FAC sets are interpreted to be produced by cyclic patterns of channel avulsion and associated drift as discussed in Part C above. **E)** Sequences and sequence stratigraphic components, and their relationship to thickening and thinning successions of FACs. From base to top, sequences are composed of a thickening (transgressive-equivalent) and thinning (highstand- to falling stage-equivalent) succession of FACs. The contact between thickening- and thinning-upward FACs is interpreted as the maximum-flooding equivalent. Thickening-upward FACs are characterized by multistory channel sand bodies at the base, abundant overbank mudrock at the top, and relatively immature, more poorly-drained paleosols throughout. Thinning-upward FACs are characterized by overbank mudrock at the base and increasingly common channel sand bodies at the top, and more mature, well-drained paleosols throughout. Sequence boundaries are underlain by the most mature and well-drained paleosols. **F)** Schematic accommodation profile labeled with corresponding sequence stratigraphic components. Two shorter-period eustatic cycles are superimposed on a longer-period episode of rapid subsidence.

sequently has more of geologic time accounted for through deposition than weathering (*sensu* Posamentier and Allen 1993). If so, then what otherwise would have been evidence for composite pedogenesis at a sequence boundary would instead be recorded as a thinning-upward succession of FACs that are each overlain by discrete paleosols that become increasingly mature and well-drained up-section. The preservation of such high-frequency alluvial depositional events and intervening periods of exposure would be unlikely in a lower accommodation setting. High rates of subsidence are also supported by the preservation of highstand-equivalent strata, which are more likely removed by erosion in low-accommodation settings (Boyd et al. 2000). The interpretation of rapid subsidence during deposition of the Dawson Creek interval is possibly contradicted by the sequence-scale, somewhat ''sawtooth pattern'' of paleosol maturity and drainage that is considered by Retallack (1998) as characteristic of low sedimentation rates and incomplete stratal successions (Figs. 3, 9). The ''sawtooth pattern'' observed at Dawson Creek, however, is inconclusive. Sequence-scale trends of paleosol maturity and drainage are arguably as irregular as they are ''sawtooth'' in nature (Fig. 3). Furthermore, Dawson Creek sequences range from approximately 90 to 110 m in thickness, whereas the sequences depicted by Retallack (1998, his fig. 6.6, p. 152) average only 10 m in thickness.

Second, perhaps third-order episodes of tectonic uplift caused ''falling stage'' to ''lowstand'' incisement that truncated out paleosol-rich ''highstand'' deposits that included composite paleosols. In such a circumstance paleosol-lean trangressive or early highstand deposits would be overlain by a surface of considerable erosional relief that may also show evidence of prolonged pedogenesis. This scenario is unlikely at Dawson Creek. No single paleosol of significantly greater maturity or better drainage was observed to be abruptly superimposed upon transgressive- or early highstand-equivalent strata at a surface of erosional truncation. Rather, the study interval has been demonstrated by Lehman (1985a, 1990) to be relatively conformable, and it contains sequences that not only include both transgressive- and highstand- to falling stage-equivalent strata but also likely correlate with third-order changes in sea level (Figs. 3, 5, 7).

Finally, pedogenesis may have occurred in a drier paleoclimate at the Dawson Creek locality than recorded during the Cenomanian of western Canada, thereby reducing the rate of pedogenesis relative to the rate of floodplain aggradation. A reduction in the rate of pedogenesis would make it less likely that paleosol ''welding'' (*sensu* Ruhe and Olson 1980) would occur along a sequence boundary during a late-highstand to falling-stage episode. Under these conditions, the stratal and pedogenic products would be similar to those described above as the first possibility; that is, thinning-upward FACs and increasingly mature and better-drained discrete paleosols associated with the late highstand to falling stage, rather than a thin, amalgamated FAC succession having composite paleosols subjacent to a sequence boundary. This idea is supported by the observation that the Dawson Creek succession lacks lacustrine and coal deposits, yet has paleosols within the transgressive-, highstand- and falling-stage-equivalent systems tracts that exhibit stage II calcic morphologies (Table 2; Fig. 6A, B). These features suggest that the Late Cretaceous and early Tertiary at Dawson Creek were characterized by a drier climate than that of the Dunvegan Formation, and therefore, likely had a concomitant reduction in the rates of pedogenesis.

CONCLUSIONS

Detailed description and analysis of the thick, age-constrained, and relatively conformable overbank-prone K–T exposures along Dawson Creek provide the following conclusions.

1. The study interval was deposited by a suspended-load fluvial system within a subhumid to perhaps semiarid climate. Outcrops are dominated by overbank mudrocks that include abundant and weakly to well-developed paleosols. Paleosols have features similar to modern Entisols, Inceptisols, Vertisols, and Alfisols.

2. Stacking-pattern analysis, traditionally used to describe and interpret composite stratal cyclicity in thick marine carbonate successions, has broader applicability to thick, relatively conformable, age-constrained alluvial successions that are dominated by overbank mudrocks.

3. The study interval is composed of a three-tier cyclic stratal hierarchy produced by the combined effects of autogenic and allogenic processes. Meter-scale fluvial aggradational cycles (FACs) are interpreted to record cyclic episodes of rapid floodplain aggradation during periods of channel avulsion, and reduced rates of sediment accumulation during periods of channel stability. Consequently, the lower parts of FACs are coarser-grained and characterized by immature paleosols, whereas the upper parts are finer-grained and commonly have a mature paleosol at their tops. Fluvial aggradational cycle sets (FAC sets) are dominated by sandstone bodies at their bases and paleosol-rich overbank mudrocks at their tops, and are thought to record a succession of channel avulsion episodes such that the channel axis periodically drifted away from and back towards a fixed position in the alluvial valley through time. Hectometer-scale fluvial sequences are disconformity-bounded stratal successions dominated by sandstone bodies at their bases and paleosol-rich overbank mudrocks at their tops, and were possibly generated in response to third-order episodes of eustatic sea-level rise and fall in the Western Interior Seaway (WIS) of North America.

4. The changing nature of fluvial facies, FAC thickness, and paleosols in hectometer-scale fluvial sequences is consistent with published conceptual and empirically based models of fluvial sequence stratigraphy. Two partial and two complete sequences are recognized at Dawson Creek. The transgressive-equivalent parts of sequences 2 and 3 have the highest proportion of channel-association sandstone facies and are further characterized by an up-section increase in the thickness of FACs that are each overlain by poorly-drained and immature paleosols. The succeeding highstand- to falling stage-equivalent succession is characterized by an up-section thinning of overbank-prone FACs that have correspondingly well-drained and mature paleosols at their tops. Sequence boundaries occur at the inflection between thinning (highstand- to falling stage-equivalent) and thickening (transgressive-equivalent) FACs.

ACKNOWLEDGMENTS

This study was supported by Baylor University URC grant #015-A02. Access to outcrops in Big Bend National Park were provided by the United States Department of the Interior via permit #BIBE-2002-SCI-0010. The manuscript benefited greatly from a pre-review by Mike Blum at the University of Nebraska. Comments provided by JSR reviewers M.J. Kraus, T.F. Lawton, P.J. McCarthy, G.C. Nadon, and J.B. Southard significantly improved the manuscript quality. This paper is dedicated to the memory of R.K. Goldhammer.

REFERENCES

AITKEN, J.F., AND FLINT, S.S., 1996, Variable expression of interfluvial sequence boundaries in the Breathitt Group (Pennsylvanian), eastern Kentucky, USA, *in* Howell, J.A., and Aitken, J.F., eds., High Resolution Sequence Stratigraphy: Innovations and Applications: Geological Society of London, Special Publication 104, p. 193–206.

ALLEN, J.R.L., 1978, Studies in fluviatile sedimentation: an exploratory quantitative model for the architecture of avulsion-controlled alluvial suites: Sedimentary Geology, v. 21, p. 129–147.

ASLAN, A., AND AUTIN, W.J., 1999, Evolution of the Holocene Mississippi River floodplain, Ferriday, Louisiana: insights of the origin of fine-grained floodplains: Journal of Sedimentary Research, v. 69, p. 800–815.

BEERBOWER, J.R., 1964, Cyclothems and cyclic depositional mechanisms in alluvial plain sedimentation, *in* Merriam, D.F., ed., Symposium on Cyclic Sedimentation: State Geological Survey of Kansas, Bulletin 169, v. II, p. 31–42.

BLAKEY, R.C., AND GUBITOSA, R., 1984, Controls on sandstone body geometry and architecture in the Chinle Formation (Upper Triassic), Colorado Plateau: Sedimentary Geology, v. 38, p. 51–86.

BLUM, M.D., AND TORNQVIST, T.E., 2000, Fluvial responses to climate and sea-level change: a review and look forward: Sedimentology, v. 47 (Suppl. 1), p. 2–48.

BOWN, T.M., AND KRAUS, M.J., 1987, Integration of channel and floodplain suites. I Developmental sequence and lateral relations of alluvial paleosols: Journal of Sedimentary Petrology, v. 57, p. 587–601.

BOYD, R., DIESSEL, C., WADSWORTH, J., CHALMERS, G., LECKIE, D., AND ZAITLIN, B., 2000, Developing a model for nonmarine sequence stratigraphy—application to the Western Canada sedimentary basin: GeoCanada 2000, Conference Abstracts, CD-ROM.

BRIDGE, J.S., 1984, Large-scale facies sequences in alluvial overbank environments: Journal of Sedimentary Petrology, v. 54, p. 583–588.

BRIDGE, J.S., AND LEEDER, M.R., 1979, A simulation model of alluvial stratigraphy: Sedimentology, v. 26, p. 617–644.

CALDWELL, W.G.E., DINER, R., EICHER, R.D., FOWLER, S.P., NORTH, B.R., STELCK, C.R., AND VON HOLDT WILHELM, L., 1993, Foraminiferal biostratigraphy of Cretaceous marine cyclothems, *in* Caldwell, W.G.E., and Kauffman, E.G., eds., Evolution of the Western Interior Basin: Geological Association of Canada, Special Paper 39, p. 477–520.

CANT, D.J., 1998, Sequence stratigraphy, subsidence rates, and alluvial facies, Mannville Group, Alberta foreland basin, *in* Shanley, K.W., and McCabe, P.J., eds., Relative Role of Eustasy, Climate and Tectonism in Continental Rocks: SEPM, Special Publication 59, p. 49–63.

CHAPPELL, J., OMURA, A., EZAT, T., MCCULLOCH, M., PANDOLFI, J., OTA, Y., AND PILLANS, B., 1996, Reconciliation of late Quaternary sea-levels derived from coral terraces at Huon Peninsula with deep sea oxygen isotope records: Earth and Planetary Science Letters, v. 141, p. 227–236.

COSUNA, 1983, Southwest/southwest mid-continent region stratigraphic correlation chart, *in* Hills, J.M., and Kottlowski, F.E., regional coordinators, Correlation of Stratigraphic Units of North America (COSUNA) Project: American Association of Petroleum Geologists, Tulsa, Oklahoma, chart.

DAVIDOFF, A.J., AND YANCEY, T.E., 1993, Eustatic cyclicity in the Paleocene and Eocene: data from the Brazos River Valley, Texas: Tectonophysics, v. 222, p. 371–395.

DRUMMOND, C.N., AND WILKINSON, B.H., 1993, On the use of cycle thickness diagrams as records of long-term sea level change during accumulation of carbonate sequences: Journal of Geology, v. 101, p. 687–702.

ETHRIDGE, F.G., WOOD, L.J., AND SCHUMM, S.A., 1998, Cyclic variables controlling fluvial sequence development: problems and perspectives, *in* Shanley, K.W., and McCabe, P.J., ed., Relative Role of Eustasy, Climate, and Tectonism in Continental Rocks: SEPM, Special Publication 59, p. 17–29.

GRADSTEIN, F.M., AGTERBERG, F.P., OGG, J.G., HARDENBOL, J., VAN VEEN, P., THIERRY, J., AND

HUANG, Z., 1994, A Mesozoic time scale: Journal of Geophysical Research, v. 99, p. 24,051–24,074.

HAQ, B.U., HARDENBOL, J., AND VAIL, P.R., 1988, Mesozoic and Cenozoic chronostratigraphy and cycles of sea-level change, *in* Wilgus, C.K., Hastings, B.S., Kendall, C.G.St.C., Posamentier, H.W., Ross, C.A., and Van Wagoner, J.C., eds., Sea-Level Changes: An Integrated Approach: SEPM, Special Publication 42, p. 71–108.

HELLER, P.L., AND PAOLA, C., 1996, Downstream changes in alluvial architecture: an exploration of controls on channel-stacking patterns: Journal of Sedimentary Research, v. 66, p. 297–306.

HOLBROOK, J.M., 1996, Complex fluvial response to low gradients at maximum regression: a genetic link between smooth sequence-boundary morphology and architecture of overlying sheet sandstone: Journal of Sedimentary Research, v. 66, p. 713–722.

KAUFFMAN, E.G., 1977, Geological and biological overview: Western Interior Cretaceous basin: The Mountain Geologist, v. 14, p. 75–99.

KAUFFMAN, E.G., 1984, Paleobiogeography and evolutionary response dynamic in the Cretaceous Western Interior Seaway of North America, *in* Westermann, G.E.G., ed., Jurassic–Cretaceous Biochronology and Paleogeography of North America: Geological Association of Canada, Special Paper 27, p. 273–306.

KRAUS, M.J., 1987, Integration of channel and floodplain suites, II. Vertical relations of alluvial paleosols: Journal of Sedimentary Petrology, v. 57, p. 602–612.

KRAUS, M.J., 1999, Paleosols in clastic sedimentary rocks: their geologic applications: Earth-Science Reviews, v. 47, p. 41–70.

KRAUS, M.J., 2002, Basin-scale changes in floodplain paleosols: implications for interpreting alluvial architecture: Journal of Sedimentary Research, v. 72, p. 500–509.

KRAUS, M.J., AND ASLAN, A., 1993, Eocene hydromorphic paleosols: significance for interpreting ancient floodplain processes: Journal of Sedimentary Petrology, v. 63, p. 453–463.

KRAUS, M.J., AND ASLAN, A., 1999, Palaeosol sequences in floodplain environments: a hierarchical approach, *in* Thiry, M., and Simon-Coincon, R., eds., Palaeoweathering, Palaeosurfaces and Related Continental Deposits: International Association of Sedimentologists, Special Publication 27, p. 303–321.

LEGARRETA, L., AND ULIANA, M.A., 1998, Anatomy of hinterland depositional sequences: Upper Cretaceous fluvial strata, Neuquen Basin, west-central Argentian, *in* Shanley, K.W., and McCabe, P.J., eds., Relative Role of Eustasy, Climate, and Tectonism in Continental Rocks: SEPM, Special Publication 59, p. 83–92.

LEHMAN, T.M., 1985a, Stratigraphy, sedimentology, and paleontology of Upper Cretaceous (Campanian–Maastrichtian) sedimentary rocks in Trans-Pecos Texas [Ph.D. dissertation]: The University of Texas at Austin, 299 p.

LEHMAN, T.M., 1985b, Transgressive–regressive cycles and environments of coal deposition in Upper Cretaceous strata of the Trans-Pecos Texas: Gulf Coast Association of Geological Societies, Transactions, v. 35, p. 431–438.

LEHMAN, T.M., 1986, Late Cretaceous sedimentation in Trans-Pecos Texas, *in* Pause, P.H., and Spears, R.G., eds., Geology of the Big Bend Area and Solitario Dome, Texas: West Texas Geological Society, Fieldtrip Guidebook, no. 86–82, p. 105–110.

LEHMAN, T.M., 1989, Upper Cretaceous (Maastrichtian) paleosols in Trans-Pecos Texas: Geological Society of America, Bulletin, v. 101, p. 188–203.

LEHMAN, T.M., 1990, Paleosols and the Cretaceous/Tertiary transition in the Big Bend region of Texas: Geology, v. 18, p. 363–364.

LEHMAN, T.M., 1991, Sedimentation and tectonism in the Laramide Tornillo Basin of West Texas: Sedimentary Geology, v. 75, p. 9–28.

LEHRMANN, D.J., AND GOLDHAMMER, R.K., 1999, Secular variation in parasequence and facies stacking patterns of platform carbonates: a guide to application of stacking-pattern analysis in strata of diverse ages and settings, *in* Harris, P.M., Saller, A.H., and Simo, J.A., eds., Advances in Carbonate Sequence Stratigraphy: Application to Reservoirs, Outcrops and Models: SEPM, Special Publication 63, p. 187–225.

LILLEGRAVEN, J.A., AND OSTRESH, L.M., JR., 1990, Late Cretaceous (earliest Campanian/Maastrichtian) evolution of western shorelines of the North American Western Interior Seaway in relation to known mammalian faunas: Geological Society of America, Special Paper 243, 30 p.

MARTINSEN, O.J., RYSETH, A., HELLAND-HANSEN, W., FLESCHE, H., TORKILDSEN, G., AND IDEL, S., 1999, Stratigraphic base level and fluvial architecture: Ericson Sandstone (Campanian), Rock Springs Uplift, SW Wyoming, USA: Sedimentology, v. 47, p. 235–259.

MCBRIDE, E.F., WEIDIE, A.E., WOLLEBEN, J.A., AND LAUDON, R.C., 1974, Stratigraphy and structure of the Parras and La Popa Basins, Northeastern Mexico: Geological Society of America, Bulletin, v. 85, p. 1603–1622.

MCCARTHY, P.J., AND PLINT, A.G., 1998, Recognition of interfluve sequence boundaries: integrating paleopedology and sequence stratigraphy: Geology, v. 26, p. 387–390.

MCCARTHY, P.J., FACCINI, U.F., AND PLINT, A.G., 1999, Evolution of an ancient coastal plain: palaeosols, interfluves and alluvial architecture in a sequence stratigraphic framework, Cenomanian Dunvegan Formation, NE British Columbia, Canada: Sedimentology, v. 46, p. 861–891.

MIALL, A.D., 1978, Lithofacies types and vertical profile models in braided river deposits: a summary, *in* Miall, A.D., ed., Fluvial Sedimentology: Canadian Society of Petroleum Geologists, Memoir 5, p. 598–604.

MILLER, K.G., BARRERA, E., OLSSON, R.K., SUGARMAN, P.J., AND SAVIN, S.M., 1999, Does ice drive early Maastrichtian eustasy?: Geology, v. 27, p. 783–786.

MORAN-ZENTENO, D., 1994, Geology of the Mexican Republic: American Association of Petroleum Geologists, Studies in Geology, no. 39, 160 p.

OLSEN, T., STEEL, R., HOGSETH, K., SKAR, T., AND ROE, S.L., 1995, Sequential architecture in a fluvial succession: sequence stratigraphy in the Upper Cretaceous Mesaverde Group, Price Canyon, Utah: Journal of Sedimentary Research, v. B65, p. 265–280.

PLINT, A.G., MCCARTHY, P.J., AND FACCINI, U., 2001, Nonmarine sequence stratigraphy: updip expression of sequence boundaries and systems tracts in a high-resolution framework, Cenomanian Dunvegan Formation, Alberta foreland basin, Canada: American Association of Petroleum Geologists, Bulletin, v. 85, p. 1967–2001.

POSAMENTIER, H.W., AND ALLEN, G.P., 1993, Siliciclastic sequence stratigraphic patterns in foreland ramp-type basins: Geology, v. 21, p. 455–458.

POSAMENTIER, H.W., AND WEIMER, P., 1993, Siliciclastic sequence stratigraphy and petroleum geology—Where to from here?: American Association of Petroleum Geologists, Bulletin, v. 77, p. 731–742.

QUIRK, D.G., 1996, ''Base profile'': a unifying concept in alluvial sequence stratigraphy, *in* Howell, J.A., and Aitken, J.F., eds., High Resolution Sequence Stratigraphy: Innovations and Applications: Geological Society of London, Special Publication 104, p. 37–49.

RAPP, S.D., MACFADDEN, B.J., AND SCHIEBOUT, J.A., 1983, Magnetic polarity stratigraphy of the early Tertiary Black Peaks Formation, Big Bend National Park, Texas: Journal of Geology, v. 91, p. 555–572.

READ, W.A., AND DEAN, J.M., 1982, Quantitative relationships between numbers of fluvial cycles, bulk lithological composition and net subsidence in a Scottish Namurian basin: Sedimentology, v. 29, p. 181–200.

RETALLACK, G.J., 1998, Fossil soils and completeness of the rock and fossil records, *in* Donovan, S.K., and Paul, C.R.C., eds., The Adequacy of the Fossil Record, Chichester, United Kingdom, Wiley, p. 133–163.

RETALLACK, G.J., 2001, Soils of the Past, Second Edition: Oxford, U.K., Blackwell Science, 404 p.

RICHARDSON, J.L., AND VEPRASKAS, M.J., 2001, Wetland Soils: Boca Raton, Florida, Lewis Publishers, 417 p.

ROBINSON-ROBERTS, L.N., AND KIRSCHBAUM, M.A., 1995, Paleogeography of the Late Cretaceous of the Western Interior of middle North America—coal distribution and sediment accumulation: U.S. Geological Survey, Professional Paper 1561, 115 p.

ROGERS, R.R., 1998, Sequence analysis of the Upper Cretaceous Two Medicine and Judith River Formations, Montana: nonmarine response to the Claggett and Bearpaw marine cycles: Journal of Sedimentary Research, v. 68, p. 615–631.

RUHE, R.V., AND OLSON, C.G., 1980, Soil welding: Soil Science, v. 130, p. 132–139.

RUNKEL, A.C., 1988, Stratigraphy, sedimentation, and vertebrate paleontology of Eocene rocks in the Big Bend region of southwest Texas [Unpublished Ph.D. dissertation]: University of Texas at Austin, Austin, Texas, 283 p.

SADLER, P.M., OSLEGER, D.A., AND MONTANEZ, I.P., 1993, On the labeling, length, and objective basis of Fischer plots: Journal of Sedimentary Petrology, v. 63, p. 360–368.

SCHIEBOUT, J.A., 1974, Vertebrate paleontology and paleoecology of Paleocene Black Peaks Formation, Big Bend National Park, Texas: Texas Memorial Museum Bulletin, 88 p.

SCHUMM, S.A., 1993, River response to baselevel change: implications for sequence stratigraphy: Journal of Geology, v. 101, p. 279–294.

SCHWANS, P., 1995, Controls on sequence stacking and fluvial to shallow-marine architecture in a foreland basin, *in* Van Wagoner, J.C., and Bertram, G.T., eds., Sequence Stratigraphy of Foreland Basin Deposits: American Association of Petroleum Geologists, Memoir 64, p. 55–102.

SHANLEY, K.W., AND MCCABE, P.J., 1993, Alluvial architecture in a sequence stratigraphic framework: a case history from the Upper Cretaceous of southern Utah, U.S.A., *in* Flint, S., and Bryant, I., eds., Quantitative Modelling of Clastic Hydrocarbon Reservoirs and Outcrop Analogs: International Association of Sedimentologists, Special Publication 15, Oxford, Blackwell Scientific Publications, p. 21–56.

SHANLEY, K.W., AND MCCABE, P.J., 1994, Perspectives on the sequence stratigraphy of continental strata: American Association of Petroleum Geologists, Bulletin, v. 78, p. 544–568.

SHELDON, N.D., AND RETALLACK, G.J., 2001, Equation for compaction of paleosols due to burial: Geology, v. 29, p. 247–250.

SOIL SURVEY DIVISION STAFF, 1993, Soil Survey Manual: Washington, D.C., U.S. Department of Agriculture, Handbook no. 18.

STANDHARDT, B.R., 1986, Vertebrate paleontology of the Cretaceous/Tertiary transition of Big Bend National Park, Texas [Unpublished Ph.D. dissertation]: Louisiana State University, Baton Rouge, Louisiana, 298 p.

STEVENS, J.B., AND STEVENS, M.S., 1989, Road logs, field trip to Big Bend region, Trans-Pecos Texas, *in* Dickerson, P.W., Stevens, M.S., and Stevens, J.B., eds., Geology of the Big Bend and Trans-Pecos Region: South Texas Geological Society, Field Trip Guidebook, 74th Annual Convention of the American Association of Petroleum Geologists, San Antonio, Texas, p. 1–72.

SUGARMAN, P.J., MILLER, K.G., BUKRY, D., AND FEIGENSON, M.D., 1995, Uppermost Campanian–Maestrichtian strontium isotopic, biostratigraphic, and sequence stratigraphic framework of the New Jersey Coastal Plain: Geological Society of America, Bulletin, v. 107, p. 19–37.

VAN WAGONER, J.C., 1995, Sequence stratigraphy and marine to nonmarine facies architecture of foreland basin strata, Book Cliffs, Utah, U.S.A., *in* Van Wagoner, J.C., and Bertram, G.T., eds., Sequence Stratigraphy of Foreland Basin Deposits: American Association of Petroleum Geologists, Memoir 64, p. 137–224.

WILSON, J.A., 1970, Vertebrate biostratigraphy of Trans-Pecos Texas: West Texas Geological Society, Publication 71-59, p. 159–166.

WOLLEBEN, J.A., MCBRIDE, E.F., AND WEIDIE, A.E., 1970, Geology of the La Popa area, *in* McBride, E.F., Weidie, A.E., and Wolleben, J., eds., 1970 Spring Field Trip, Hidalgo Canyon–La Popa Valley, Nuevo Leon, Mexico: Corpus Christi Geological Society, Spring Field Conference, p. 59–66.

WRIGHT, V.P., AND MARRIOTT, S.B., 1993, The sequence stratigraphy of fluvial depositional systems: the role of floodplain sediment storage: Sedimentary Geology, v. 86, p. 203–210.

YOSHIDA, S., WILLIS, A., AND MIALL, A.D., 1996, Tectonic control of nested sequence architecture in the Castlegate Sandstone (Upper Cretaceous), Book Cliffs, Utah: Journal of Sedimentary Research, v. 66, p. 737–748.

Received 11 December 2002; accepted 22 October 2003.